Indian Journal of Pure & Applied Physics
Vol. 59, June 2021, pp. 452-455

Investigation on BST-NZF Magnetoelectric Composites

Vishal Khatri[a], Vinay Kumar[b], Ashwani Kumar[c], Shravan Kumar Meena[d] & Renu Rani*[e]

[a]Department of Physics, Nalanda College of Engineering, Chandi, Nalnda, Bihar, India- 803 101
[b]Department of Physics, COBS&H, CCS Haryana Agricultural University, Hisar, Haryana, India- 125 004
[c]Nanoscience laboratory Institute Instrumentation Centre, IIT Roorkee, India-247 667
[d]Department of Physics, Motilal Nehru College, University of Delhi, South Campus, New Delhi-110 021
[e]P.G. Department of Physics, Magadh University, Bodhgaya, Bihar, INDIA-824234

Received 28 September 2020; accepted 12 February 2021

Here, we are reporting electrical properties of Barium Titanate and Ni-Zn ferrite magneto-electric composites. Sr substituted barium titanate (BST = 90%) and MnO_2 doped nickel zinc ferrite (NZF = 10%) were selected as individual phases for magneto-electric composite. Individual $Ba_{0.9}Sr_{0.1}TiO_3$ and $Ni_{0.8}Zn_{0.2}Fe_2O_4$ were prepared separately through solid state reaction route. For structural analysis, the sintered samples subjected to X-ray diffraction reveal a presence of both the ferrite and ferroelectric phase in the composite sample. Dielectric properties were measured as a function of frequency and temperature. Curie temperature for pure BST was observed to be 92 °C, whereas in the composite sample, the transition became broader. P-E hysteresis loops were recorded at 20 Hz for all the samples.

Keywords: Barium Titanate; BST; Ni-Zn ferrite; composites

1Introduction

Magnetoelectric effect is the coupling between electrical and magnetic properties of a material, such materials where (ME) is intrinsic are known as magneto electic. In addition to the physics involved, such materials find several applications, viz. information storage, spintronics, *etc*. Single phase materials have their limiting use in practical devices because magnetoelectric (ME) effect is considerably weak even at low temperature. The alternatives are magnetoelectric composites because they exhibit large value of ME coefficient[1]. Ferrite and ferroelectric are constituent phases of these composites. They can be exploited as waveguides, sensors, phase shifter, modulators and memory devices *etc.* [2,3]. Limited data is available in the literature "on investigation of dielectric and ferroelectric properties of ferroelectro-magnetic composites". In view of this, in the present work $Ba_{0.9}Sr_{0.1}TiO_3$ is selected as a ferroelectric phase due to its high dielectric constant, relatively low dielectric loss and variable Curie temperature depending on the concentration of strontium[4], $Ni_{0.8}Zn_{0.2}Fe_2O_4$ is selected as a ferrite phase because it is one of the most versatile well known spinel magnetic material due to its high resistivity and low eddy current losses[5]. The Saturation magnetization of nickel ferrite increases with zinc content, hence its magnetoelectric coefficient increases. MnO_2 was added to minimize the hopping mechanism $Fe^{2+} \leftrightarrow Fe^{3+}$ which results in an increase in the resistivity of the samples. In nickel ferrite, conductivity is mainly due to hopping between $Fe^{2+} \leftrightarrow Fe^{3+}$ [6]. In this paper, we present the detailed report on dielectric properties of the prepared composites. From this study we can get the valuable information about the mechanism of electrical conduction and dielectric polarization in the prepared composites.

2 Experimental Work

The individual phases (ferrite and ferroelectric) were prepared by conventional solid state reaction method. AR grade NiO, ZnO, Fe_2O_3 were used as raw materials for synthesis of ferrite phase. The mixing process was carried out by ball-milling using zirconia balls and distilled water as milling media. The slurry was dried and calcined in alumina crucible at 1000 °C for 4 hrs. To the calcined powder, a small amount (0.5% by weight) of MnO_2 was added, ball milled and recalcined at 1000 °C for 4 hours. The recalcined powder was then ball milled again and dried. The ferroelectric phase was prepared using the same route by using AR grade $BaCO_3$, $SrCO_3$ and TiO_2 as raw materials and calcined at 1100 °C. The composite was

*Corresponding author: (E-mail: renudhy@gmail.com)

prepared by mixing 10% by wt. $Ni_{0.80}Zn_{0.20}Fe_2O_4$ (NZF) phase to the $Ba_{0.90}Sr_{0.10}TiO_3$ (BST) (90% by wt.) phase. The mixing process was carried out by ball-milling using zirconia balls and distilled water as milling media. After drying, small amount of diluted PVA was added as binder and the pellets having 2-3mm thickness and 15 mm diameter were pressed using the uniaxial hydraulic press. The pellets were sintered at 1325 °C for 4hrs. A constant heating rate of 5 °C/min was chosen to achieve this temperature. The structural characterization of the samples was carried out by using X-ray diffractometer using Cu Kα radiation (λ=1.541Å). For electrical measurement the samples were then coated with silver paste and heated in an oven at 400 °C for 1hr to ensure good ohmic contacts. The dielectric measurements were carried out as a function of frequency at different temperatures by using 4263B LCR meter interfaced to PC and programmable temperature chamber. P-E hysteresis loops were recorded at 20 Hz for all the samples.

3 Results and Discussion

The X-ray diffraction (XRD) patterns for both the samples, ferroelectric (BST) and ferroelectric-ferrite composite (BST+NZF) are shown in the Fig. 1. The pattern shows well defined peaks with specific indices which are characteristics of perovskite structure of ferroelectric phase[7]. The co-existence of the ferrite phase and ferroelectric phase is confirmed in composite sample. It is seen that there is shifting of peaks towards lower angle in case of composite which indicates that there is change in lattice parameter of ferroelectric phase. The growth of individual phases exerts stress on each other's crystal lattice and hence slight change in lattice parameter of ferroelectric phase in composite sample is expected[8].

Figure 2, shows the variation of dielectric constant with temperature at different frequencies. It is seen that dielectric constant increases with temperature up to a certain temperature called Curie temperature and after that it decreases for both the samples. In case of pure BST curie temperature is noticed at 92 °C while for composite sample the transition peak gets broadened. The room temperature dielectric constant is lowered in case of composite sample. It is seen that in case of pure BST the dielectric constant is almost independent of frequency at all the temperatures while in case of composites as the temperature approaches T_c the dielectric constant shows more dispersion in low frequency region and further increase in temperature results in a rapid decrease in dielectric constant with frequency. This shows that there is large dielectric dispersion in case of composite samples after the Curie temperature as shown in figure. In case of composites the high value of dielectric constant observed at lower frequency region is attributed to the effect of heterogeneity in the sample due to

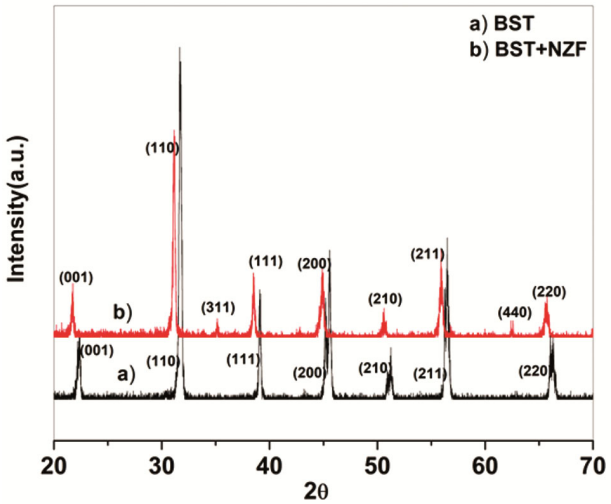

Fig. 1 — XRD patterns for the samples

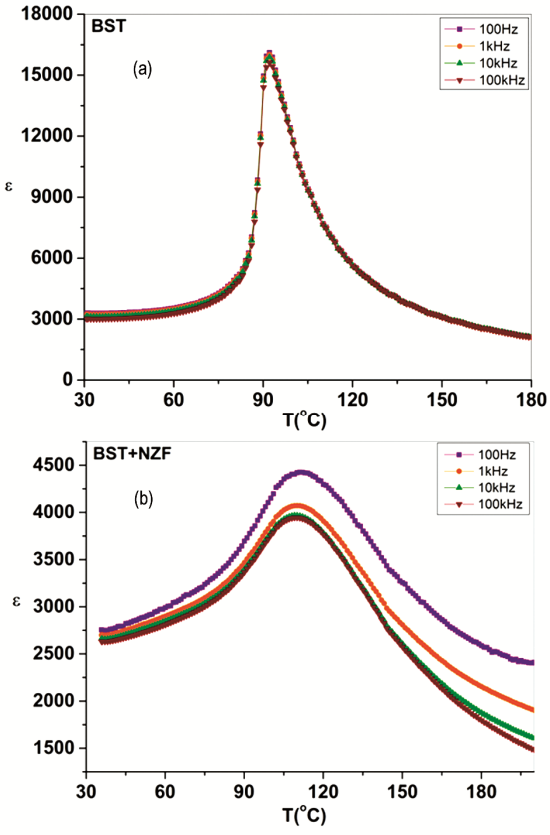

Fig. 2 — Variation of dielectric constant with temperature

simultaneous presence of two phases (ferroelectric phase as well as ferrite phase) which results in interfacial polarization in the sample at low frequency region. The value of Dielectric constant (ε), tan δ and T_c are reported in Table 1 for both the samples.

Above the Curie temperature, the temperature dependence of the dielectric constant (in paraelectric phase region) can be explained by Curie–Weiss law[9]

$$\varepsilon = \varepsilon_o + C/(T-T_o)$$

Where T_o is the Curie – Weiss temperature, ε_o is free space permittivity and C is the Curie – Weiss constant.

Figure 3 shows the variation of inverse of dielectric constant with temperature at 10 kHz for both samples. A clear deviation from the Curie–Weiss law can be seen at T_{dev} . The various parameters obtained are listed in Table 2. The value of T_o can be determined from the graph by extrapolation and values obtained are given in Table 2. It can be seen that composite samples shows diffused phase transition because composite samples follow the Curie – Weiss law at temperature higher than the T_m. The parameter δT_m describes the degree of deviation from the Curie-Weiss law and is defined as [10]

$$\delta T_m = T_{dev} - T_m$$

Where T_{dev} is the temperature at which the permittivity starts deviating from Curie-Weiss law and T_m represents the temperature of dielectric maxima.

A modified Curie-Weiss law has been proposed by many research groups to describe the diffuseness of a phase transition[11]. The degree of disorder or diffusivity (γ) for all the composition , was calculated using the expression[12]

$$\ln(1/\varepsilon - 1/\varepsilon_{max}) = \gamma \ln(T-T_c) + a$$

Where ε_{max} is the maximum value of dielectric constant at T_m. The value of γ represents the degree of diffusiveness, and it lies in the range $1 < \gamma \leq 2$, $\gamma = 1$ represents ideal Curie-Weiss behaviour, while γ between 1 and 2 indicates diffused phase transition[13]. The linear plot of $\ln(1/\varepsilon' - 1/\varepsilon'_{max})$ vs. $\ln(T-T_c)$ at 100 kHz for both the samples are shown in Fig. 4. The slopes of these plots give the parameter γ and values of γ are listed in Table 1. The value of γ for

Table 1

	γ	ε_{RT}	ε_{max}	$\tan\delta_{RT}$	$\tan\delta_{max}$	P_r ($\mu C/cm^2$)	P_r/P_s	E_c (kV/cm)
BST	1.19	3010	15624	0.026	0.050	6.85	0.33	2.192
BST+NZF	1.66	2630	3945	0.011	0.007	1.28	0.12	1.48

Table 2

	BST		BST+NZF	
	1kHz	100kHz	1kHz	100kHz
T_m(°C)	92	92	110	110
T_o (°C)	81	85	58	73
T_{dev} (°C)	99	106	128	130
δT_m(°C)	7	14	128	130

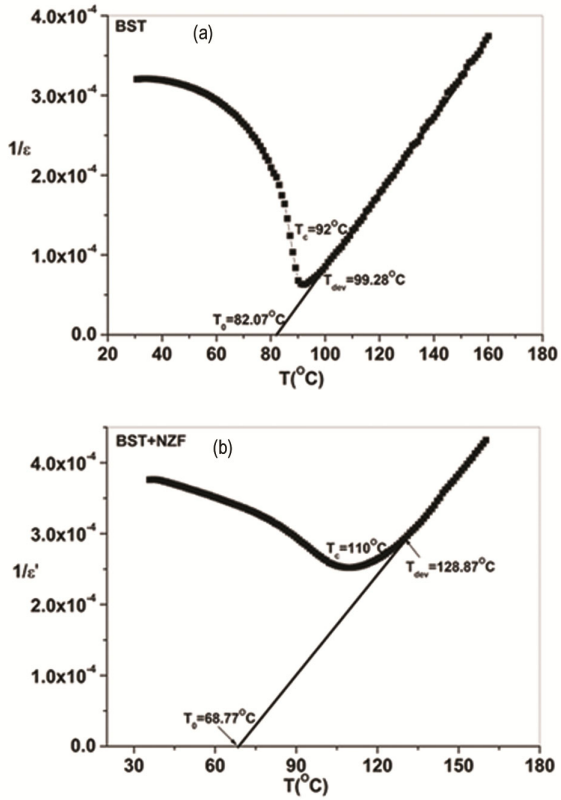

Fig. 3 — The inverse of ε as a function of temperature at 10 kHz for both samples

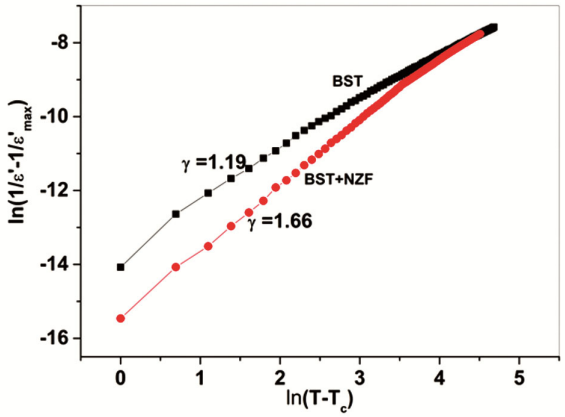

Fig. 4 — $\ln(1/\varepsilon' - 1/\varepsilon'_{max})$ *vs.* $\ln(T-T_c)$ for both the samples at 100 kHz

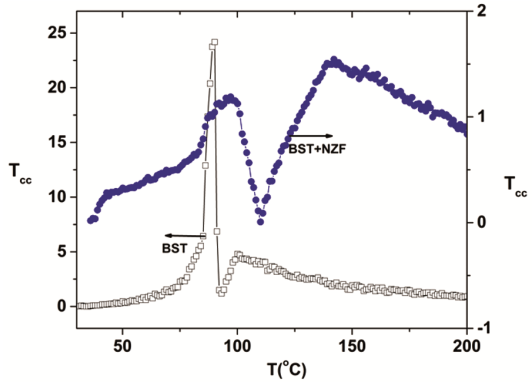

Fig. 5 — T_{cc} *Vs*. temperature at 100 kHz for both samples

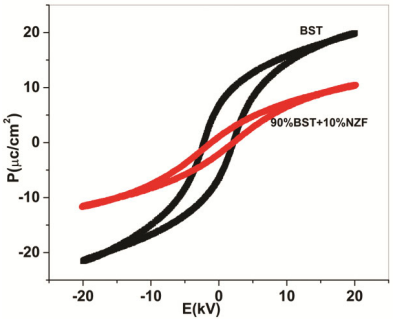

Fig. 6 — P-E hysteresis loop at room temperature

composite sample approaches 2. This indicates diffused phase transition. It is found that the value of γ is higher in case of composite samples. In composite samples more diffused phase transition and more deviation from Curie-Weiss law may be assumed due to structural disordering. The structural disorder in the samples arises due to the presence of different phases (Ferroelectric and Non-ferroelectric regions) and number of voids. This suggests a microscopic heterogeneity in the compound with different local Curie points which results in broadening of transition peak in composites[14].

The temperature coefficients of capacitance was calculated by using the formula shown below[15].

$$T_{cc} = ((C_T - C_{T-1})/ C_{T-1})*100$$

Figure 5 shows the graph between the T_{cc} versus temperature. The low value of T_{cc} for composite sample also confirmed a diffuse phase transition.

Figure 6 shows the room temperature P-E loops for both the samples. The hysteresis measurements reveal that the value of remnant polarization (P_r) of the composite samples decreases and it relates to low internal polarizabilities, strain, electromechanical coupling and electro-optic activity[16]. The low degree of loop squareness ratio (P_r/ P_s) of P-E loop is also observed in case of composite sample. This indicates inhomogeneous non uniform grains in ferroelectric phase due to presence of ferrite phase. The value of P_r, P_r/P_s and E_c are given in Table 1.

4 Conclusion

XRD pattern for both the samples show well defined peaks. The co-existence of ferrite phase and ferroelectric phase is confirmed from XRD in composite sample. The dielectric peak gets suppressed and become broadened with the addition of ferrite content. The composite sample obeys Curie-Weiss law at temperature much higher than T_m. The dielectric dispersion is more in case of composite sample. The value of P_r and P_r/P_s ratio is less in composite sample.

References

1 Nan C W, *Phys Rev B*, 50 (1994) 6082.
2 Bracke L P M & van Vliet RG, *Int J Electron*, 51 (1981) 255.
3 Wan J G, Liu J M, Chand H L W, Choy C L, Wang G H & Nan C W, *J Appl Phys*, 93 (2003) 9916.
4 Abdelkefi H, Khemakhem H, Vélu G, Carru J C & Von Der Mühll R, *J Alloys Compd*, 399 (2005) 1.
5 Cheng Y, Zheng Y, Wang Y, Bao F & Qin Y, *J Solid State Chem*, 178 (2005) 2394.
6 Waser R, *Adv Mater*, 4 (1992) 698.
7 Cross L E, *Ferroelectrics*,151 (1994) 305.
8 Fawzi A S, Sheikh A D & Mathe V L, *Phys B Condens Matter*, 405 (2010) 340.
9 Lines M E & Glass A M, *Principles and Applications of Ferroelectrics and Related Materials*, Oxford University Press, 2010.
10 Tang X G, Chew K H & Chan H L W, *Acta Mater*, 52 (2004) 5177.
11 Eric Cross L, *Ferroelectrics*,76 (1987) 241.
12 Pilgrim S M, Sutherland A E & Winzer S R, *J Am Ceram Soc*, 73 (1990) 3122.
13 Prasad K, *Indian J Eng Mater Sci*, 7 (2000) 446.
14 Kumar P, Singh S, Juneja J K, Prakash C & Raina K K, *Phys B Condens Matter*,404 (2009) 2126.
15 Dixit A, Majumder S B, Katiyar R S & Bhalla A S, *Appl Phys Lett*, 82 (2003) 2679.
16 Williamsont G K & Hallt W H, *X-Ray Line Broadening from Filed Aluminium and Wolfram**.